

## Anti-*Mycobacterium tuberculosis* and Cytotoxicity Activities of Ruthenium(II)/Bipyridine/Diphosphine/Pyrimidine-2-thiolate Complexes: The Role of the Non-Coordinated N-Atom

Benedicto A. V. Lima,<sup>a</sup> Rodrigo S. Corrêa,<sup>a,b</sup> Angelica E. Graminha,<sup>a</sup> Aleksey Kuznetsov,<sup>a</sup> Javier Ellena,<sup>c</sup> Fernando R. Pavan,<sup>d</sup> Clarice Q. F. Leite<sup>d</sup> and Alzir A. Batista<sup>\*,a</sup>

<sup>a</sup>Departamento de Química, Universidade Federal de São Carlos,  
CP 676, 13565-905 São Carlos-SP, Brazil

<sup>b</sup>Departamento de Química, Instituto de Ciências Exatas e Biológicas (ICEB),  
Universidade Federal de Ouro Preto, 35400-000 Ouro Preto-MG, Brazil

<sup>c</sup>Instituto de Física de São Carlos, Universidade de São Paulo,  
CP 780, 13560-970 São Carlos-SP, Brazil

<sup>d</sup>Departamento de Ciências Biológicas, Faculdade de Ciências Farmacêuticas,  
Universidade Estadual Paulista (Unesp), 14800-900 Araraquara-SP, Brazil

The [Ru(Spym)(bipy)(P-P)]PF<sub>6</sub>, [Spym = pyrimidine-2-thiolate anion; P-P = 1,2-*bis*(diphenylphosphino)ethane, 1,3-*bis*(diphenylphosphino)propane and 1,1'-*bis*(diphenylphosphino)ferrocene] complexes were synthesized and characterized by spectroscopic, electrochemical and elemental analysis, and by X-ray crystallography. The minimal inhibitory concentration (MIC) of the compounds against *Mycobacterium tuberculosis* and the complex concentration causing 50% tumor cell growth inhibition (IC<sub>50</sub>) against breast cancer cells, MDA-MB-231, were determined. All three compounds gave promising values in both tests. It is interesting to mention that all three complexes display MICs against *Mycobacterium tuberculosis* showing higher activity than cycloserine, a second line drug used in the treatment of the illness. The complexes interact weakly with the DNA.

**Keywords:** ruthenium complexes, pyrimidine-2-thiolate, diphosphine ligand, cytotoxicity, tuberculosis

### Introduction

Ruthenium is widely studied due to its versatility and potential applications in several fields of the science.<sup>1-4</sup> In general, ruthenium complexes can have their properties tuned, since slight changes in the coordination environment around the metal center lead to significant alterations of their electrochemical, spectroscopic and chemical behavior, and hence their biological activity, which explains the interest in these compounds.<sup>5,6</sup> In the same way, thiopyrimidines have attracted special attention in the last two decades for their biochemical interactions, being useful ligands because of their analogy to purine and pyrimidine nucleobases.<sup>7-9</sup> Thiopyrimidines and their derivatives have been investigated for their potential antiviral, antibacterial, fungicidal, and

antithyroid activity, and as well as for their photochemical properties.<sup>10-13</sup> Building on their pharmaceutical properties, the thiopyrimidines can have synergic effects when coordinated to metals,<sup>14,15</sup> since they can bind to metals in a variety of coordination modes: neutral monodentate, bidentate, as bridge ligands and anionic monodentate, and also bridging two metallic centers by nitrogen and sulfur atoms.<sup>16-23</sup> Phosphine ligands have both  $\sigma$ -donor and  $\pi$ -acceptor character, being able to stabilize metals in both high and low oxidation states.<sup>24</sup> In addition, biphosphine (P-P) ligands also play an important role in catalysis and in bioinorganic chemistry,<sup>25,26</sup> and together with the 2,2'-bipyridine (bipy) ligand, eventually could contribute to increase biological activities and DNA interactions. Therefore, the aim of this work is to synthesize and to characterize ruthenium(II) complexes with general formula [Ru(Spym)(bipy)(P-P)]PF<sub>6</sub> [Spym = pyrimidine-2-thiolate

\*e-mail: daab@ufscar.br

anion; P–P = 1,2-*bis*(diphenylphosphino) ethane = dppe (**1**), 1,3-*bis*(diphenylphosphino)propane = dppp (**2**), and 1,1'-*bis*(diphenylphosphino)ferrocene = dppf (**3**), and to study their anti-*M. tuberculosis* (MTB) and cytotoxicity activities against human breast cancer cells (MDA-MB-231) and against the health cell line from mice (L929 cell line).

## Experimental

### Materials and measurements

Solvents were purified by standard methods. All chemicals used were of reagent grade or comparable purity.  $\text{RuCl}_3 \cdot 3\text{H}_2\text{O}$  and the ligands 1,2-*bis*(diphenylphosphino) ethane, 1,3-*bis*(diphenylphosphino)propane, 1,1'-*bis*(diphenylphosphino)ferrocene, 2,2'-bipyridine and pyrimidine-2-thiolate were used as received from Aldrich.

All nuclear magnetic resonance (NMR) experiments were performed at 20 °C on a Bruker spectrometer, 9.4 T, observing  $^1\text{H}$  at 400.13 MHz and  $^{31}\text{P}\{^1\text{H}\}$  at 161.98 MHz. The NMR spectra were recorded in  $\text{CDCl}_3$  or  $(\text{CD}_3)_2\text{CO}$ , with tetramethylsilane (TMS) ( $^1\text{H}$ ) and 85%  $\text{H}_3\text{PO}_4$  ( $^{31}\text{P}\{^1\text{H}\}$ ) as internal and external references, respectively. The  $^{31}\text{P}\{^1\text{H}\}$  NMR spectra of the complexes were also recorded in dimethylsulfoxide (DMSO) and in the same solutions in which the DNA binding were carried out (5 mmol  $\text{L}^{-1}$  tris(hydroxymethyl)aminomethane (Tris)-HCl and 50 mmol  $\text{L}^{-1}$  NaCl, pH 7.4), and in these cases the complexes **1**, **2** and **3** showed to be stable for at least for 72 h. The splitting of proton and phosphorus resonances, respectively, in the reported  $^1\text{H}$  and  $^{31}\text{P}\{^1\text{H}\}$  NMR spectra is labeled as s = singlet, d = doublet, t = triplet and m = multiplet. UV-Vis spectra were recorded on HP8452A (diode array) spectrophotometer. The infrared (IR) spectra were recorded from KBr sample pellets in a Bomem-Michelson 102 FTIR spectrometer, in the range 4000-200  $\text{cm}^{-1}$ . Conductivity (presented as  $\Omega^{-1} \text{cm}^2 \text{mol}^{-1}$ ) was measured in  $\text{CH}_2\text{Cl}_2$  with a Micronal B-330 connected to a Pt cell of constant 0.089  $\text{cm}^{-1}$ ; measurements were made at 25 °C on  $10^{-3} \text{mol L}^{-1}$  solutions of the complexes. Cyclic voltammetry experiments were carried out at 25 °C in  $\text{CH}_2\text{Cl}_2$  containing 0.10 mol  $\text{L}^{-1}$   $\text{Bu}_4\text{NClO}_4$  (TBAP) (Fluka Purum), with a Bioanalytical Systems Inc. BAS-100B/W electrochemical analyzer. The working and auxiliary electrodes were stationary Pt foils; a Luggin capillary probe was used and the reference electrode was Ag/AgCl. Under these conditions, the ferrocene is oxidized at 0.43 V (Fc<sup>+</sup>/Fc). The microanalyses were performed in the Microanalytical Laboratory at the Chemistry Department of the Federal University of São Carlos, with an EA 1108 CHNS microanalyzer (Fisons Instruments).

### Anti-*M. tuberculosis* activity assay

The anti-MTB activity of the compounds was determined by the resazurin microtiter assay (REMA).<sup>27</sup> Stock solutions of the test compounds were prepared in DMSO and diluted in Middlebrook 7H9 broth (Difco), supplemented with oleic acid, albumin, dextrose and catalase (OADC enrichment, BBL/Becton Dickinson), to obtain final drug concentrations from 0.15 to 250  $\mu\text{g mL}^{-1}$ . The serial dilutions were carried out in a Precision XS Microplate Sample Processor (Biotek<sup>TM</sup>). Isoniazid was dissolved in distilled water, according to the manufacturers' recommendations (Difco), and used as a standard drug. MTB H<sub>37</sub>Rv (American Type Culture Collection (ATCC) 27294) was grown at 37 °C for 7 to 10 days in Middlebrook 7H9 broth supplemented with OADC, plus 0.05% Tween 80 to avoid clumps. Cultures were centrifuged for 15 min at 3,150 × g, washed twice, suspended in phosphate-buffered saline and aliquots were frozen at -80 °C. After 2 days, the number of colony-forming units (CFU) was determined. MTB H<sub>37</sub>Rv (ATCC 27294) was thawed and mixed in microplate wells with the test compounds and 7H9 broth, yielding a final testing volume of 200  $\mu\text{L}$  with  $2 \times 10^4$  CFU  $\text{mL}^{-1}$ . Microplates were incubated for 7 days at 37 °C, after which resazurin was added for the reading. Wells that turned from blue to pink, with the development of fluorescence, indicated growth of bacterial cells, while maintenance of the blue color indicated bacterial inhibition.<sup>27,28</sup> The fluorescence was read (530 nm excitation filter and 590 nm emission filter) in a SPECTRAfluor Plus (Tecan<sup>®</sup>) microfluorimeter. The minimal inhibitory concentration (MIC) was defined as the lowest concentration resulting in 90% inhibition of growth of MTB.<sup>28</sup> As a standard test, the MIC of isoniazid was determined on each microplate. The acceptable range of isoniazid MIC is from 0.015 to 0.06  $\mu\text{g mL}^{-1}$ .<sup>27,28</sup> Each test was set up in triplicate.

### *In vitro* cytotoxicity

The *in vitro* cytotoxicity assays on cultured human tumor cell lines still represent the standard method for the initial screening of antitumor agents. Thus, as a first step in assessing their pharmacological properties, the new ruthenium complexes were assayed against human breast tumor cell lines MDA-MB-231 and L929 (ATCC:CCL 1, mouse fibroblast). The cells were routinely maintained in Dulbecco's modified Eagle's medium (DMEM) supplemented with 10% fetal bovine serum (FBS), at 37 °C in a humidified 5% CO<sub>2</sub> atmosphere. After reaching confluence, the cells were detached by trypsinization and counted. For the cytotoxicity assay,  $5 \times 10^4$  cells  $\text{well}^{-1}$  were

seeded in 200  $\mu\text{L}$  of complete medium in 96-well assay microplates (Corning Costar). The plates were incubated at 37  $^{\circ}\text{C}$  in 5%  $\text{CO}_2$  for 24 h to allow cell adhesion, prior to drug testing. All tested compounds were dissolved in sterile DMSO (stock solution with maximum concentration of 20  $\text{mmol L}^{-1}$ ) and diluted to 5, 2, 1, 0.5, 0.2, 0.02 and 0.002  $\text{mmol L}^{-1}$ . From each of these dilute samples, 2  $\mu\text{L}$  aliquots were added to 200  $\mu\text{L}$  medium (without FBS) giving a final concentration of DMSO of approximately 1% and a final concentration of the complex diluted about 100 $\times$ . Attached cells were exposed to the compounds for a 24 h. Cell respiration, as an indicator of cell viability, was then determined by the mitochondrial-dependent reduction of 3-(4,5-dimethylthiazol-2-yl)-2,5-diphenyltetrazolium bromide (MTT).<sup>29</sup> MTT solution (0.5  $\text{mg mL}^{-1}$ ) was added to cell cultures and incubated for 3 h, after which 100  $\mu\text{L}$  of isopropanol was added to dissolve the precipitated formazan crystals. The conversion of MTT to formazan by metabolically viable cells was monitored in an automated microplate reader at 570 nm. The cell viability percentage was calculated by dividing the average absorbance of the cells treated with the test compounds by that of the control; cell viability percentage was plotted against drug concentration (logarithmic scale) to determine the drug concentration at which 50% of the cells are viable relative to the control ( $\text{IC}_{50}$ ), the error being estimated for the average of 3 trials.

#### DNA interaction studies

All the measurements on DNA were carried out in Tris-HCl buffer (5  $\text{mmol L}^{-1}$  Tris-HCl and 50  $\text{mmol L}^{-1}$  NaCl, pH 7.4). In order to compare the DNA binding affinities quantitatively, the intrinsic binding constants  $K_b$  of complexes **1-3** bound to calf thymus (CT)-DNA were found by monitoring the changes in absorbance of the  $\pi \rightarrow \pi^*$  spectral band (253-275 nm) with increasing concentration of DNA and using equation 1:<sup>30</sup>

$$[\text{DNA}] / (\epsilon_a - \epsilon_f) = [\text{DNA}] / (\epsilon_b - \epsilon_f) + 1 / K_b (\epsilon_b - \epsilon_f) \quad (1)$$

where  $[\text{DNA}]$  is the concentration of DNA in base pairs, the apparent absorption coefficients  $\epsilon_a$ ,  $\epsilon_f$  and  $\epsilon_b$  correspond to  $A_{\text{obs}} / [\text{complex}]$ , the extinction coefficient for the free ruthenium complex and the extinction coefficient for the free complex in the fully bound form, respectively. In the plot of  $[\text{DNA}] / (\epsilon_a - \epsilon_f)$  vs.  $[\text{DNA}]$ , the value of  $K_b$  is given by the ratio of slope to intercept. The concentration *per* nucleotide was determined by absorption spectrophotometric analysis, assuming the molar absorption coefficient 6600  $\text{mol}^{-1} \text{L cm}^{-1}$  at 260 nm.<sup>31</sup>

#### X-Ray crystallography

Crystals of the three compounds were grown by slow evaporation of dichloromethane/methanol or dichloromethane/diethyl ether solutions. The crystals were mounted on a goniometer in an Enraf-Nonius kappa geometry charge-coupled device (CCD) diffractometer with graphite monochromated Mo  $K\alpha$  ( $\lambda = 0.71073 \text{ \AA}$ ) radiation. The final unit cell parameters were based on all reflections. Data were collected at room temperature with the COLLECT program, and integration and scaling of the reflections were performed with the HKL Denzo-Scalepack software package.<sup>32,33</sup> Absorption correction was carried out by the Gaussian method.<sup>34</sup> The structures were solved by direct methods with SHELXS-97.<sup>35</sup> The models were refined by full-matrix least squares on F2 by means of SHELXL-97.<sup>36</sup> All hydrogen atoms were stereochemically positioned and refined with a riding model. The Oak Ridge thermal ellipsoid plot (ORTEP) views were prepared with ORTEP-3 for Windows.<sup>37</sup> Hydrogen atoms on the aromatic rings were refined isotropically, each with a thermal parameter 20% greater than the equivalent isotropic displacement parameter of the atom to which it is bound.

#### Theoretical calculations

The geometry optimization of complex **3** was performed using the Gaussian 09 package, employing the hybrid B3LYP density functional<sup>38</sup> and Los Alamos double-zeta effective core potential (LanL2dz) with the associated basis sets.<sup>38-40</sup> This approach is further referred to as B3LYP/LanL2dz. The geometry optimization was followed by the vibrational frequencies calculation using the same approach. In order to estimate the contributions of specific atoms to the HOMO and LUMO of the complex studied, we performed calculations of fragment densities of states (projected densities of states, PDOS), using the keywords 'Fragment' and 'Population' as implemented in the Gaussian 09 program. For the PDOS calculations we used the B3LYP/LanL2dz optimized geometry and the approach designated as B3LYP/[Ru,Fe:CEP-121G; C,H,O,N,P:6-31G\*], with the Stevens/Basch/Krauss effective core potential triple-split basis (CEP-121G) on Ru and Fe atoms and the split-valence 6-31G\* basis set on the light atoms.<sup>41,42</sup> The last approach was shown to provide good agreement with the experimental data.

#### Synthesis of the complexes

*cis*-[RuCl<sub>2</sub>(bipy)(dppe)] and *cis*-[RuCl<sub>2</sub>(bipy)(dppp)]

The synthesis of the precursor *cis*-[RuCl<sub>2</sub>(bipy)(dppe)] has already been reported, but here another method

was used.<sup>43</sup> A suspension of 428 mg (0.502 mmol) of *cis*-[RuCl<sub>2</sub>(PPh<sub>3</sub>)<sub>2</sub>(bipy)] was heated to reflux for 10 min, in CH<sub>2</sub>Cl<sub>2</sub> and then 246 mg (0.618 mmol) of dppe was added. After 30 min the color of the suspension changed from golden to dark red. The mixture was kept in reflux for 24 h and a very small amount of a fine powder was formed, which was removed by filtration and the limp dark red resulting solution was refluxed for 30 min longer. The volume of the solution was reduced to ca. 3 mL and diethyl ether was added to precipitate the complex, which was filtered off and washed with diethyl ether (2 × 5 mL) and hexane (2 × 5 mL) and dried under vacuum. Yield: 83%; anal. calcd. for C<sub>36</sub>H<sub>32</sub>N<sub>2</sub>Cl<sub>2</sub>P<sub>2</sub>Ru: C, 59.51; H, 4.44; N, 3.86%; found: C, 59.86; H, 4.52; N, 3.90%; <sup>31</sup>P{<sup>1</sup>H} NMR (161.98 MHz, CH<sub>2</sub>Cl<sub>2</sub>) δ 68.0 and 61.0 (<sup>2</sup>J<sub>P-P</sub> 54.0 Hz).

Also, the precursor *cis*-[RuCl<sub>2</sub>(bipy)(dppp)] was synthesized in the same way as the complex *cis*-[RuCl<sub>2</sub>(bipy)(dppe)]. Yield: 85%; anal. calcd. for C<sub>37</sub>H<sub>34</sub>N<sub>2</sub>Cl<sub>2</sub>P<sub>2</sub>Ru: C, 60.01; H, 4.62; N, 3.78%; found: C, 59.95; H, 4.57; N, 3.89%; <sup>31</sup>P{<sup>1</sup>H} NMR (161.98 MHz, CH<sub>2</sub>Cl<sub>2</sub>) δ 37.7 and 29.8 (<sup>2</sup>J<sub>P-P</sub> 42.1 Hz)

#### *cis*-[RuCl<sub>2</sub>(bipy)(dppf)]

This complex was synthesized as reported in the literature.<sup>44</sup> Dppf (499 mg, 0.566 mmol) was added to a solution of [RuCl<sub>2</sub>(PPh<sub>3</sub>)<sub>3</sub>] (542.5 mg, 0.566 mmol), in 50 mL CH<sub>2</sub>Cl<sub>2</sub>. The color of the solution changed from purple-black to red, within a few minutes. The solution was stirred for 30 min and bipy (88.4 mg, 0.566 mmol) was added. After 30 min of stirring, the solvent was reduced to about 2 mL and 15 mL of diethyl ether were added. The precipitated complex was filtered off, washed twice with ether (2 × 5 mL) and then dried under vacuum. Yield: 90%; anal. calcd. for C<sub>44</sub>H<sub>36</sub>N<sub>2</sub>Cl<sub>2</sub>P<sub>2</sub>FeRu: C, 59.89; H, 4.08; N, 3.17%; found: C, 60.01; H, 4.10; N, 3.25%; <sup>31</sup>P{<sup>1</sup>H} NMR (161.98 MHz, CH<sub>2</sub>Cl<sub>2</sub>) δ 41.8 and 36.2 (<sup>2</sup>J<sub>P-P</sub> 36.0 Hz).

#### [Ru(Spym)(bipy)(dppe)]PF<sub>6</sub> (**1**) and [Ru(Spym)(bipy)(dppp)]PF<sub>6</sub> (**2**)

HSpym (11.2 mg, 0.100 mmol) and NH<sub>4</sub>PF<sub>6</sub> (24.5 mg, 0.150 mmol) were added to a solution of the precursor *cis*-[RuCl<sub>2</sub>(bipy)(dppe)] (72.5 mg, 0.100 mmol) or *cis*-[RuCl<sub>2</sub>(bipy)(dppp)] (74 mg, 0.100 mmol) in 20 mL CH<sub>2</sub>Cl<sub>2</sub>, and the mixture was allowed to react under reflux in an argon atmosphere for 24 h. The final mixtures were concentrated to ca. 2 mL and 15 mL diethyl ether were added to precipitate the products of the reactions, which were filtered off, washed with water (2 × 10 mL) and diethyl ether (2 × 10 mL), and dried under vacuum.

Yield **1**: 89%; IR (KBr)  $\nu_{\max}$  / cm<sup>-1</sup> 3053, 2920, 1603, 1558, 1539, 1483, 1469, 1433, 1309, 1252, 1159, 1101, 1001, 841, 758, 750, 702, 676, 652, 557, 526, 501, 488, 447, 426; <sup>1</sup>H NMR (400 MHz, (CD<sub>3</sub>)<sub>2</sub>CO) δ 9.34 (m, 1H, bipy), 8.49 (d, 1H, *J* 8.4 Hz, bipy), 8.40 (d, 1H, *J* 8.4 Hz, bipy), 8.30 (d, 1H, *J* 5.6 Hz, bipy), 8.18 (dd, 1H, *J* 4.6 and 2.4 Hz, Spym), 8.14 (dt, 1H, *J* 8.0 and 1.6 Hz, bipy), 7.98 (dt, 2H, *J* 8.0 and 1.6 Hz, bipy), 7.63-7.37 (m, 1H, Spym; 1H, bipy; 10H, Ph), 7.32-7.26 (m, 1H, Ph), 7.19 (dt, 3H, *J* 7.6 and 1.6 Hz, Ph), 7.15-7.07 (m, 1H, bipy; 2H, Ph), 6.96 (dt, 2H, *J* 6.0 and 1.6 Hz, Ph), 6.71 (dt, 1H, *J* 5.0 and 1.2 Hz, Spym), 6.65-6.58 (m, 2H, Ph), 3.37-2.60 (m, 1H, CH<sub>2</sub>), 3.70-3.42 (m, 1H, CH<sub>2</sub>), 3.13-2.97 (m, 1H, CH<sub>2</sub>), 2.95-2.79 (m, 1H, CH<sub>2</sub>);  $\Lambda_M$  / (Ω<sup>-1</sup> cm<sup>2</sup> mol<sup>-1</sup>) 19.47; anal. calcd.: C, 52.69; H, 3.86; N, 6.14; S, 3.51%; found: C, 52.77; H, 4.02; N, 6.20; S, 3.18%.

Yield **2**: 86%; IR (KBr)  $\nu_{\max}$  / cm<sup>-1</sup> 3068, 2972, 2874, 1603, 1581, 1527, 1485, 1468, 1435, 1309, 1269, 1159, 1093, 999, 844, 765, 754, 698, 665, 655, 557, 514, 507, 489, 426; <sup>1</sup>H NMR (400 MHz, CDCl<sub>3</sub>) δ 8.99 (d, 1H, *J* 6.4 Hz, bipy), 8.63 (m, 1H, bipy), 8.53 (d, 1H, *J* 8.4 Hz, bipy), 8.26 (d, 1H, *J* 6.0 Hz, bipy), 8.19 (t, 1H, *J* 7.6 Hz, bipy), 7.84 (dd, 1H, *J* 6.4 and 2.4 Hz, Spym), 7.70 (t, 1H, *J* 6.8 Hz, bipy), 7.45 (t, 1H, *J* 8.4 Hz, bipy), 7.35-7.18 (m, 1H, Spym; 5H, Ph), 7.17-7.06 (m, 1H, bipy; 6H, Ph), 6.96 (t, 2H, *J* 7.2 Hz, Ph), 6.93-6.81 (m, 5H, Ph), 6.74-6.67 (m, 2H, Ph), 6.20 (t, 1H, *J* 4.8 Hz, Spym), 3.47 (m, 1H, CH<sub>2</sub>), 2.96 (m, 1H, CH<sub>2</sub>), 2.47 (m, 2H, CH<sub>2</sub>), 2.32 (m, 2H, CH<sub>2</sub>);  $\Lambda_M$  / (Ω<sup>-1</sup> cm<sup>2</sup> mol<sup>-1</sup>) 19.49; anal. calcd.: C, 53.64; H, 4.40; N, 5.82; S, 3.33%; found: C, 53.38; H, 5.01; N, 6.03; S, 3.11%.

#### [Ru(Spym)(bipy)(dppf)]PF<sub>6</sub> (**3**)

The complex [Ru(Spym)(bipy)(dppf)]PF<sub>6</sub> (**3**) was synthesized in a similar way to **1** and **2**, but in this case triethylamine (0.15 mmol) was added to the reaction solution, and reflux was not necessary. Yield: 90%; IR (KBr)  $\nu_{\max}$  / cm<sup>-1</sup> 3055, 2924, 2850, 1602, 1562, 1543, 1481, 1469, 1433, 1309, 1253, 1159, 1091, 1041, 1000, 841, 762, 750, 698, 636, 557, 545, 518, 499, 489, 445, 432; <sup>1</sup>H NMR (400 MHz, (CD<sub>3</sub>)<sub>2</sub>CO) δ 9.26 (d, 1H, *J* 5.6 Hz, bipy), 8.66 (d, 1H, *J* 7.6 Hz, bipy), 8.53 (m, 1H, bipy), 8.37 (d, 1H, *J* 8.0 Hz, bipy), 8.31 (t, 1H, *J* 7.6 Hz, bipy), 7.95-7.87 (1H, Spym; m, 2H, Ph), 7.83 (t, 1H, *J* 6.8 Hz, bipy), 7.65 (1H, *J* 7.2 Hz, bipy), 7.55 (t, 1H, *J* 6.0 Hz, Spym), 7.50-7.36 (m, 4H, Ph), 7.30 (m, 1H, bipy), 7.24-7.10 (m, 7H, Ph), 7.00-6.90 (m, 4H, Ph), 6.82 (t, 2H, *J* 8.8 Hz, Ph), 6.79-6.72 (m, 1H, Ph), 6.25 (t, 1H, *J* 4.8 Hz, Spym), 6.02 (m, 1H, Cp), 4.97 (s, 1H, Cp), 4.74 (m, 1H, Cp), 4.53 (m, 1H, Cp), 4.33-4.25 (m, 3H, Cp), 3.50 (m, 1H, Cp);  $\Lambda_M$  / (Ω<sup>-1</sup> cm<sup>2</sup> mol<sup>-1</sup>) 18.81; anal. calcd.: C, 53.75; H, 3.81; N, 5.17; S, 2.96%; found: C, 53.53; H, 3.92; N, 5.33; S, 2.71%.

## Results and Discussion

### Synthesis and characterization

The easy reactivity of the  $[\text{RuCl}_2(\text{bipy})(\text{P}-\text{P})]$  precursors allowed the syntheses of complexes with general formula  $[\text{Ru}(\text{Spym})(\text{bipy})(\text{P}-\text{P})]\text{PF}_6$  by substitution of both chloride ions by the  $\text{Spym}^-$  ligand (Scheme 1).

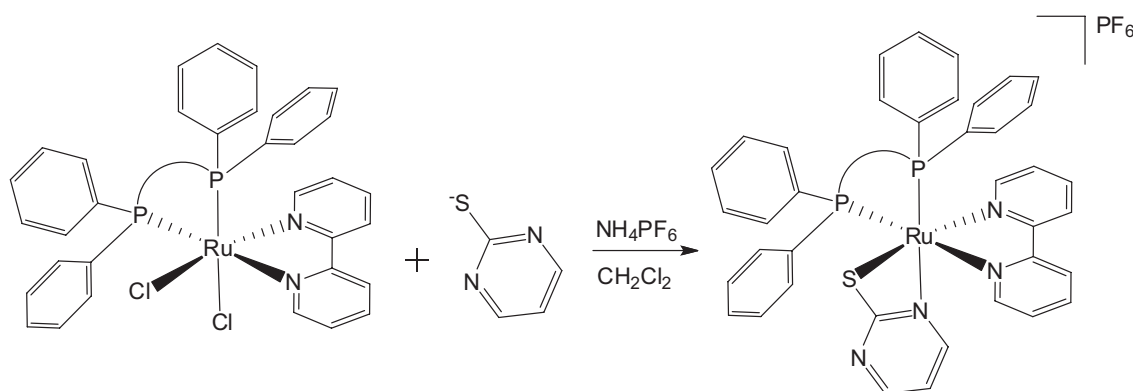
The  $^{31}\text{P}\{^1\text{H}\}$  NMR spectra of the compounds showed typical AX spin systems characterized by the nuclear magnetic nonequivalence of the two phosphorus atoms present in the complexes. The values of the chemical shifts obtained for the complexes **1-3** and for the precursors are given in Table 1. All the compounds exhibited septets whose chemical shift was centered at  $\delta -144$  ppm, indicating the presence of  $\text{PF}_6^-$  as the counter-ion. As expected, the doublets shown by the complexes  $[\text{Ru}(\text{Spym})(\text{bipy})(\text{P}-\text{P})]\text{PF}_6$  are upshifted relative to the precursors, indicating that the chlorine ligands in the precursors shield the phosphorus atoms of the phosphines more efficiently than the coordinated  $\text{Spym}^-$  ligand (Table 1).

The  $^1\text{H}$  NMR spectra of the compounds show a series of multiplets, ranging from  $\delta$  7.68 to 6.38, corresponding to the 20 hydrogen atoms of the diphosphine phenyl rings. The eight hydrogen atoms of bipy are observed in the  $\delta$  9.50-6.87 region, and some of the signals overlap with the proton resonances of the phenyl groups. The protons corresponding to the  $-(\text{CH}_2)_n-$  groups of the phosphines

appeared as multiplets in the  $\delta$  3.37-2.53 region for **1** and  $\delta$  3.47-1.81 for **2**. The three protons of Spym show their chemical shifts in the  $\delta$  8.18-6.20 region. For the  $[\text{Ru}(\text{Spym})(\text{bipy})(\text{dppf})]\text{PF}_6$  complex **3** the ferrocene hydrogens show resonances between  $\delta$  6.02 and 3.50, corresponding to eight hydrogen atoms. The six peaks observed for these protons are caused by the non-equivalence of the phosphorus atoms bonded to the cyclopentadienyl rings (Cp), as confirmed by a pair of doublets observed in the  $^{31}\text{P}\{^1\text{H}\}$  NMR spectrum of the  $[\text{Ru}(\text{Spym})(\text{bipy})(\text{dppf})]\text{PF}_6$  complex.

The compounds **1-3** were studied by cyclic voltammetry technique, and it was found that they show one  $\text{Ru}^{\text{II}}/\text{Ru}^{\text{III}}$  redox pair: complex **1** shows a *quasi-reversible* process,  $E_{1/2} = 0.99$  V, and complex **2** one *quasi-reversible* redox pair,  $E_{1/2} = 1.00$  V (see Table 1). Complex **3**, which is a bimetallic compound, exhibits two processes: the first is also *quasi-reversible* ( $E_{1/2} = 0.77$  V) and relates to  $\text{Ru}^{\text{II}}/\text{Ru}^{\text{III}}$ , while the second, irreversible, with  $E_{\text{pa}} = 1.28$  V, belongs to the  $\text{Fe}^{\text{II}}/\text{Fe}^{\text{III}}$  oxidation process (Figure 1).

To confirm this suggestion, a few drops of the salt  $\text{NH}_4\text{SCN}$ , dissolved in methanol were added to the electrochemical cell. The typical red color of the " $\text{Fe}^{3+}\text{-SCN}^-$ " species on the electrode surface appeared only when the potential reached about 1.2 V, showing that at this point, indeed, the iron(II) of the dppf ligand was being oxidized. This also shows that the iron(II) of the dppf ligand is stabilized by its coordination to the ruthenium(II) center. In complexes *fac*- $[\text{RuCl}_3(\text{NO})(\text{dppf})]$  and



**Scheme 1.** Reaction of syntheses of the  $[\text{Ru}(\text{Spym})(\text{bipy})(\text{P}-\text{P})]\text{PF}_6$  complexes, where P-P means dppe (for complex **1**), dppp (for complex **2**) and dppf (for complex **3**).

**Table 1.**  $^{31}\text{P}\{^1\text{H}\}$  NMR and cyclic voltammetry data of the compounds

Complex	$\delta$ $^{31}\text{P}\{^1\text{H}\}$ / ppm	$^2J_{\text{P-P}}$ / Hz	$E_{\text{pa}}$ / V	$I_{\text{pa}}/I_{\text{pc}}$
$[\text{Ru}(\text{Spym})(\text{bipy})(\text{dppe})]\text{PF}_6$ ( <b>1</b> )	72.4 and 70.3	20.2	1.07	1.53
$[\text{Ru}(\text{Spym})(\text{bipy})(\text{dppp})]\text{PF}_6$ ( <b>2</b> )	39.0 and 31.8	47.7	1.11	0.99
$[\text{Ru}(\text{Spym})(\text{bipy})(\text{dppf})]\text{PF}_6$ ( <b>3</b> )	50.4 and 45.3	46.9	0.86/1.28 <sup>a</sup>	1.45/-

<sup>a</sup>Refers to  $\text{Fe}^{\text{III}}/\text{Fe}^{\text{II}}$  process.  $\delta$ : Chemical shift;  $^2J_{\text{P-P}}$ : two bond P-P coupling constant;  $E_{\text{pa}}$ : anodic peak potential;  $I_{\text{pa}}/I_{\text{pc}}$ : anodic peak current/cathodic peak current ratio.

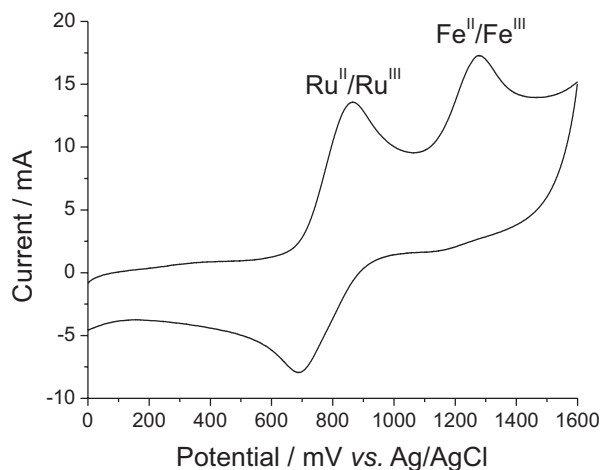


**Figure 1.** Cyclic voltammogram of the complex **3** ( $\text{CH}_2\text{Cl}_2$ ,  $0.1 \text{ mol L}^{-1}$  TBAP, scan rate  $100 \text{ mV s}^{-1}$ ).

$[\text{Ru}(\eta^6\text{-C}_{10}\text{H}_{14})(\text{dppf})\text{Cl}]\text{PF}_6$ , the iron(II) was oxidized at 1.0 and 0.86 V, respectively.<sup>10,45</sup> In the case of  $[\text{Ru}(\eta^6\text{-C}_{10}\text{H}_{14})(\text{dppf})\text{Cl}]\text{PF}_6$  there is probably a competitive effect acting to make the oxidation of the iron(II) easier than in the complex  $[\text{Ru}(\text{Spym})(\text{bipy})(\text{dppf})]\text{PF}_6$ .<sup>46,47</sup>

The PDOS calculations performed for the complex **3** showed the contributions of the Fe and Ru d-orbitals in the complex, HOMO equal to 48 and 16%, respectively. These results reinforce the assignment of the oxidation processes observed for the complex **3** in its cyclic voltammograms, where the first oxidation process was assigned to the ruthenium(II) and the second oxidation process was assigned to the iron(II).

All the electrochemical processes mentioned above involve one electron, as was shown by electrolytic measurements.

### Structural study

X-Ray structures of the compounds are represented in Figure 2. Data collection and experimental details are summarized in Table 2, and selected bond distances and angles are presented in Table 3. All the compounds show distorted geometry around the ruthenium center with one phosphorus atom positioned *trans* to the nitrogen atom of the ligand HSpym (P1 *trans* to N1) and the other phosphorus atoms *trans* to one nitrogen of the bipyridine (P2 *trans* to N4). Thus, in all three complexes the sulfur atom is positioned *trans* positioned to the nitrogen atom (N3) of the 2,2'-bipyridine ligand.

The Ru–P and Ru–N bond distances lie within the normal range usually found for ruthenium complexes containing tertiary phosphines as ligands.<sup>48–50</sup> In the new complexes the Ru–P (*trans* to the nitrogen atom of Spym) bond lengths are shorter than the Ru–P distances (*trans* to

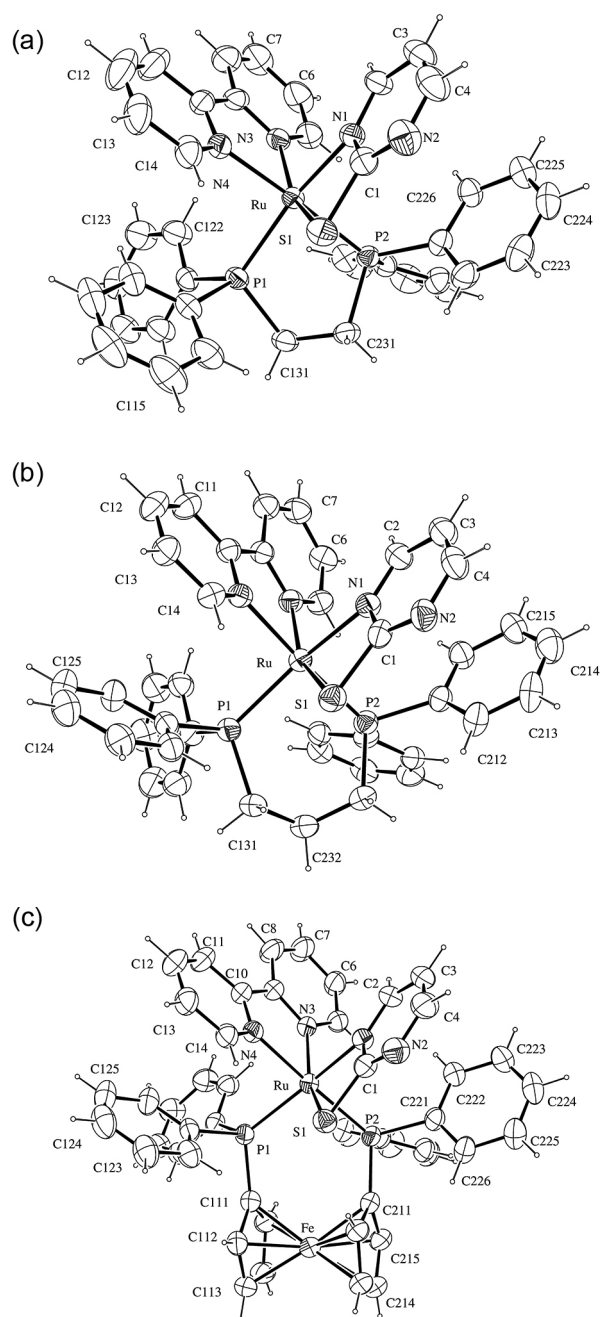


**Figure 2.** The molecular structures of (a)  $[\text{Ru}(\text{Spym})(\text{bipy})(\text{dpe})]\text{PF}_6$ ; (b)  $[\text{Ru}(\text{Spym})(\text{bipy})(\text{dpp})]\text{PF}_6$  and (c)  $[\text{Ru}(\text{Spym})(\text{bipy})(\text{dppf})]\text{PF}_6$ . The selected atoms are labeled and ellipsoids are drawn at the 30% probability level.

the nitrogen atoms of bipy). Ru–P distances of P–P follow the order:  $\text{dppf} > \text{dppp} > \text{dpe}$ . The P–Ru–P angles are comparable to the values previously observed for this kind of complex.<sup>49,50</sup>

To stabilize the crystal structure of the complexes **1–3**, there are weak C–H...F–P and C–H...N–C intermolecular interactions, as well as  $\pi$ – $\pi$  stacking and van der Waals forces. Interestingly, the crystal structure of the complex **3** forms infinite hydrophobic channels formed by the dppf

**Table 2.** Crystal data and refinement parameters for complexes **1-3**

Complex	<b>1</b>	<b>2</b>	<b>3</b>
Empirical formula	[C <sub>40</sub> H <sub>35</sub> N <sub>4</sub> P <sub>2</sub> SRu] PF <sub>6</sub>	[C <sub>41</sub> H <sub>32</sub> N <sub>4</sub> P <sub>2</sub> SRu]PF <sub>6</sub> ·½(C <sub>4</sub> H <sub>10</sub> O)	[C <sub>48</sub> H <sub>39</sub> N <sub>4</sub> P <sub>2</sub> SFeRu]PF <sub>6</sub> ·½(CH <sub>3</sub> OH)
Formula weight	911.76	962.85	1083.74
Crystal system	orthorhombic	orthorhombic	monoclinic
Space group	P2 <sub>1</sub> 2 <sub>1</sub> 2 <sub>1</sub>	Pnaa	C2/c
Unit cell dimensions / Å	a = 11.9615(1) b = 15.2742(2) c = 21.4786(3)	a = 18.5895(11) b = 20.3401(15) c = 21.9190(14)	a = 33.4315(8) b = 17.5844(5) c = 20.9225(5) β = 123.501(1)°
Volume / Å <sup>3</sup>	3924.19(8)	8287.8(9)	10256.5(5)
Z	4	8	8
Density (calculated) / (mg m <sup>-3</sup> )	1.543	1.543	1.404
Absorption coefficient / mm <sup>-1</sup>	0.639	0.611	0.771
F(000)	1848	3928	4392
Crystal size / mm <sup>3</sup>	0.27 × 0.16 × 0.12	0.22 × 0.20 × 0.03	0.43 × 0.31 × 0.26
θ Range / degree	3.14 to 26.73	2.94 to 25.0	2.92 to 26.49
Index ranges	-15 ≤ h ≤ 14 -19 ≤ k ≤ 19 -26 ≤ l ≤ 27	-18 ≤ h ≤ 21 -23 ≤ k ≤ 23 -23 ≤ l ≤ 25	-41 ≤ h ≤ 39 -22 ≤ k ≤ 22 -26 ≤ l ≤ 26
Reflections collected	29335	42262	35825
Independent reflection	8300 [R(int) = 0.0332]	7049 [R(int) = 0.0995]	10459 [R(int) = 0.0877]
Completeness to θ / %	99.4	98.5	98.4
Maximum and minimum transmission	0.933 and 0.872	0.979 and 0.886	0.843 and 0.721
Data / restraint / parameter	8300 / 0 / 552	7049 / 0 / 530	10459 / 1 / 598
S	1.047	1.055	1.006
Final R indices [I > 2σ(I)]	R1 = 0.0321 wR2 = 0.0795	R1 = 0.0669 wR2 = 0.1472	R1 = 0.0574 wR2 = 0.1496
R indices (all data)	R1 = 0.0423 wR2 = 0.0842	R1 = 0.1165 wR2 = 0.1695	R1 = 0.0853 wR2 = 0.1684
ρ <sub>max</sub> and ρ <sub>min</sub> / (e Å <sup>-3</sup> )	0.383 and -0.437	0.503 and -0.696	0.809 and -1.397

Z: number of formula units per cell; F(000): zero-order structure factor; S: goodness-of-fit on F<sub>2</sub>; ρ<sub>max</sub> and ρ<sub>min</sub>: largest diff. peak and hole.

moiety (Figure 3). This channel is filled by disordered methanol molecules that act as guest solvent, displaying an important role for crystal self-assembly stabilization. In general, the host-guest systems are stabilized by non-covalent interactions such as depicted in Figure 3.

#### Vibrational spectra

The IR spectra of all three complexes confirm the presence of the Spym<sup>-</sup> ligand coordinated to the metal. The band assigned to the ν(N-H) vibration, which appears at 3200-3100 cm<sup>-1</sup> in free thiones, is absent in the spectra of the complexes, indicating that the ligand is coordinated to the metal in the deprotonated form.<sup>51,52</sup> Bands from the coordinated Spym<sup>-</sup> ligand appear at approximately 1570 and

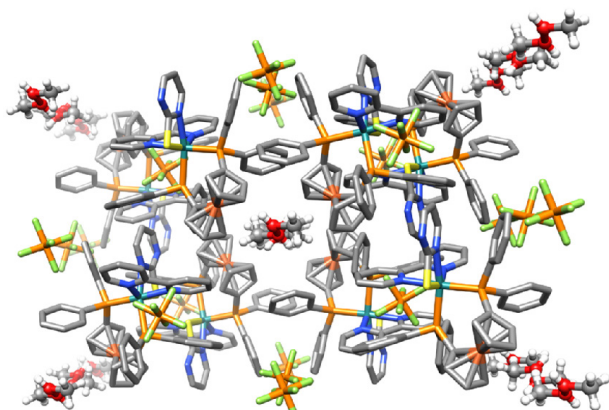
1549 cm<sup>-1</sup> (ν(C=C) + ν(C=N)), 1434 cm<sup>-1</sup> (ν(N=C) + δ(CH)) and at 1375 and 1159 cm<sup>-1</sup> (ν(C=S)) for all three complexes. Also, bands present in the spectra in the region 690-740 cm<sup>-1</sup> can be assigned as ν(C=S).<sup>53-56</sup>

#### Electronic spectra

Electronic spectra of the three complexes were obtained in dichloromethane and in DMSO solutions and the results are listed in Table 4. The transitions found for all three complexes are at about 290 nm (ε ca. 30000 mol<sup>-1</sup> L cm<sup>-1</sup>) and 420 nm (ε ca. 4000 mol<sup>-1</sup> L cm<sup>-1</sup>), corresponding to intraligand (IL) and metal-ligand charge transfer (MLCT) transitions, respectively. The electronic spectra of structurally similar ruthenium complexes containing

**Table 3.** Selected bond distances and bond angles of complexes **1-3**

Complex	<b>1</b>	<b>2</b>	<b>3</b>
Bond distance / Å			
Ru–P(1)	2.2888(11)	2.2933(19)	2.3413(10)
Ru–P(2)	2.2963(10)	2.2981(18)	2.3308(10)
Ru–N(1)	2.119(4)	2.122(5)	2.129(3)
Ru–N(3)	2.109(4)	2.113(5)	2.127(3)
Ru–N(4)	2.123(4)	2.136(5)	2.142(3)
Ru–S(1)	2.4074(11)	2.4026(18)	2.4165(10)
S(1)–C(1)	1.743(5)	1.720(7)	1.731(4)
Fe–C (average)	–	–	2.041(4)
Bond angle / degree			
N(3)–Ru–N(1)	89.63(11)	90.2(2)	89.63(11)
N(3)–Ru–N(4)	76.58(12)	77.3(2)	76.58(12)
N(1)–Ru–N(4)	84.69(11)	84.0(2)	84.69(11)
N(3)–Ru–P(2)	104.07(8)	100.73(16)	104.07(8)
N(1)–Ru–P(2)	92.32(9)	93.48(15)	92.32(9)
N(4)–Ru–P(2)	176.95(8)	176.82(15)	176.95(8)
N(3)–Ru–P(1)	101.01(8)	108.17(15)	101.01(8)
N(1)–Ru–P(1)	165.86(9)	160.46(16)	165.86(9)
N(4)–Ru–P(1)	88.71(8)	93.26(15)	88.71(8)
N(3)–Ru–S(1)	155.27(8)	156.98(15)	155.27(8)
P(2)–Ru–S(1)	86.76(4)	87.72(6)	86.76(4)
P(1)–Ru–S(1)	100.29(3)	93.10(7)	100.29(3)

**Figure 3.** Crystal self-assembly of the complex **3** viewed along the *c*-axis, showing the hydrophobic channel.**Table 4.** Data from electronic spectra of complexes **1-3** in dichloromethane

Complex	IL	MLCT
	$\lambda_{\max}$ / nm ( $\epsilon$ / (mol <sup>-1</sup> L cm <sup>-1</sup> ))	$\lambda_{\max}$ / nm ( $\epsilon$ / (mol <sup>-1</sup> L cm <sup>-1</sup> ))
[Ru(Spym)(bipy)(dppe)]PF <sub>6</sub> ( <b>1</b> )	292 (32570)	410 (4665)
[Ru(Spym)(bipy)(dppp)]PF <sub>6</sub> ( <b>2</b> )	290 (32613)	420 (4120)
[Ru(Spym)(bipy)(dppf)]PF <sub>6</sub> ( <b>3</b> )	292 (29479)	416 (3841)

IL: intraligand transition; MLCT: metal-ligand charge transfer transition;  $\lambda_{\max}$ : wavelength of maximum absorption;  $\epsilon$ : molar absorption coefficient.

diphosphine and diimine ligands show bands in the visible region, close to 400 nm, which were assigned as MLCT transitions.<sup>57-60</sup>

#### Cytotoxicity against MDA-MB-231 cell lines

The MDA-MB-231 tumor cancer cells and L929 mouse cells were exposed to each complex and to the free ligands, for a period of 24 h, in order to allow them to reach the DNA or any other biological target. As a positive control, the cytotoxicity of cisplatin was assessed under the same experimental conditions. The IC<sub>50</sub> values, calculated from the dose-survival curves generated by the MTT assays performed after the drug treatment, are shown in Table 5. It can be seen that the free ligands were inactive against either the tumor cell or the mouse cell line.

All three new complexes are very active against MDA-MB-231 breast human tumor cells showing low values of IC<sub>50</sub> and high values of IC<sub>50</sub> against normal L929 cells. The high activity of complexes **1-3** gives support to our previous suggestion that a non-coordinated atom, in this case, the nitrogen (N2) atom of the Spym<sup>-</sup> ligand, can allow interaction of the complexes with DNA or another biomolecule, increasing the cytotoxicity of the complexes. The good results obtained for similar complexes with 4,6-dimethyl-2-mercaptopyridine also support this suggestion.<sup>53</sup>

#### Anti-mycobacterial activity

The compounds were investigated for their *in vitro* anti-mycobacterial activity against *M. tuberculosis* strain H37Rv, by the microplate Alamar Blue assay (MABA) method.<sup>27</sup> The MICs found for the ruthenium complexes **1-3**, free ligands and isoniazid are shown in Table 5. According to these tests, the compounds exhibited promising activity, with MIC values in the range 1.56-4.12 mg mL<sup>-1</sup>, lower than those of cycloserine (MIC 12.5-50.0 mg L<sup>-1</sup>), a second-line drug used in several schemes of conventional tuberculosis treatment.<sup>58</sup> As can be seen in Table 5 the MIC values for free ligands were much higher than those observed for the complexes **1-3**.

**Table 5.** IC<sub>50</sub> and MIC values of complexes **1-3**, free ligands and reference drugs, measured in 1.0% DMSO solutions

Complex	IC <sub>50</sub> / $\mu\text{M}$		H37Rv		SI
	MDA-MB-231	L929	MIC / ( $\text{mg mL}^{-1}$ )	MIC / ( $\mu\text{M mL}^{-1}$ )	IC <sub>50</sub> / MIC
<b>1</b>	0.53 $\pm$ 0.41	60.3 $\pm$ 0.3	4.12	4.5	13.4
<b>2</b>	0.35 $\pm$ 0.17	45.0 $\pm$ 0.1	1.56	1.6	28.1
<b>3</b>	0.26 $\pm$ 1.41	53.0 $\pm$ 2.7	3.12	2.9	18.3
Dppe	> 200	> 200	6.25 <sup>52</sup>	> 80	> 2.5
Dppp	> 200	> 200	> 50 <sup>53</sup>	> 121	> 1.7
Dppf	> 200	> 200	> 50	> 90	> 2.2
Bipy	> 200	> 200	25 <sup>52</sup>	160.1	> 1.2
HSpym	> 200	> 200	25	225	> 0.9
Cisplatin	2.44 $\pm$ 0.20	20.14 $\pm$ 0.19	N.M.	N.M.	N.M.
Isoniazid	N.M.	N.M.	0.03	0.22	–
Cycloserine	N.M.	N.M.	12.5-50.0	122-490	–

IC<sub>50</sub>: drug concentration at which 50% of the cells are viable relative to the control; H37Rv: *M. tuberculosis* strain; SI: selectivity index calculated by dividing IC<sub>50</sub> for the mouse cells by the MIC for the pathogen; MIC: minimal inhibitory concentration; N.M.: not measured.

In our previous publication, it was suggested that for the complex [Ru(dppb)(pic)(bipy)]PF<sub>6</sub> (pic = picolinic acid) action against *M. tuberculosis* may be in the cell wall biosynthesis, considering the differential expression of a cell wall hydrolase.<sup>61</sup> Thus, in our laboratory, research is ongoing to figure out if the diphosphine/pyrimidine-2-thiolate complexes studied in this work follow the same mechanism of action against *M. tuberculosis* previously suggested.

#### DNA binding studies

Electronic absorption spectroscopy is an effective method of examining the mode and extent of binding of a metal complex with DNA. Thus, in order to shed further light into the mode of interaction of the new compounds with DNA, experiments of absorption titration were performed, yielding the binding constants  $K_b = 1.6 \times 10^3 \text{ mol}^{-1} \text{ L}$  for **1**;  $1.3 \times 10^3 \text{ mol}^{-1} \text{ L}$  for **2** and  $1.1 \times 10^3 \text{ mol}^{-1} \text{ L}$  for **3**. All  $K_b$  values are much lower than those observed for the typical classical intercalator ethidium bromide ( $K_b = 4.94 \times 10^5 \text{ mol}^{-1} \text{ L}$  in 25 mmol L<sup>-1</sup> Tris-HCl/40 mmol L<sup>-1</sup> NaCl buffer, pH 7.9).<sup>30</sup> On the other hand,  $K_b$  found for **1-3** present the same order of magnitude comparing with some hexacoordinated ruthenium(II) complexes with *N*-heterocyclic ligands, under similar conditions.<sup>62</sup> The  $K_b$  values tendency of **1** > **2** > **3** agree with the order dppe > dppp > dppf. It suggests that the less sterically-hindered dppe in the complex **1** allows its interaction with DNA through non-coordinated nitrogen atom of the Spym ligand more effectively than **2** and **3**.

## Conclusions

Three new complexes with general formula [Ru(Spym)(bipy)(P-P)]PF<sub>6</sub>, [Spym = pyrimidine-2-thiolate; bipy = 2,2'-bipyridine; P-P = 1,2-*bis*(diphenylphosphino)ethane, 1,3-*bis*(diphenylphosphino)propane or 1,1'-*bis*(diphenylphosphino)ferrocene] were synthesized and characterized by spectroscopy, cyclic voltammetry and X-ray crystallography. The complexes exhibit low DNA binding affinity, but the *in vitro* antitumor activity test utilizing the MDA-MB-231 human tumor cell line indicated a high degree of cytotoxicity for all three complexes, better than cisplatin at the same concentration. Antimicrobial activity assays of the new complexes provided evidence that they are potential agents against *M. tuberculosis* H37Rv. The MIC values of anti-*M. tuberculosis* activity obtained for the complexes showed for them an activity higher than for cycloserine, a second line drug used in the treatment of the illness. Thus, these complexes are promising as anti-*M. tuberculosis* and antitumor drugs.

## Supplementary Information

Supplementary crystallographic data for complexes **1**, **2** and **3** (CCDC 989569, 989353 and 989390, respectively) can be obtained free of charge via <http://www.ccdc.cam.ac.uk>, or from the Cambridge Crystallographic Data Centre, 12 Union Road, Cambridge CB2 1EZ, UK; fax: +44 1223 336 033; or e-mail: deposit@ccdc.cam.ac.uk.

## Acknowledgements

This work was financially supported by CAPES, CNPq and FAPESP (Process 2012/06013-4). R. S. Correa thanks FAPESP for a postdoctoral fellowship (Process 2013/26559-4).

## References

1. Murahashi, S. I.; Takaya, H.; Naota, T.; *Pure Appl. Chem.* **2002**, *74*, 19.
2. Rodrigues, M. V. N.; Corrêa, R. S.; Vanzolini, K. L.; Santos, D. S.; Batista, A. A.; Cass, Q. B.; *RSC Adv.* **2015**, *5*, 37533.
3. Balzani, V.; Bergamini, G.; Marchioni, F.; Ceroni, P.; *Coord. Chem. Rev.* **2006**, *250*, 1254.
4. Schmid, W. F.; Zorbas-Seifried, S.; John, R. O.; Arion, V. B.; Jakupec, M. A.; Roller, A.; Galanski, M.; Chiorescu, I.; Zorbas, H.; Keppler, B. K.; *Inorg. Chem.* **2007**, *46*, 3645.
5. Delolo, F. G.; Rodrigues, C.; da Silva, M. M.; Dinelli, L. R.; Delling, F. N.; Zukerman-Schpector, J.; Batista, A. A.; *J. Braz. Chem. Soc.* **2014**, *25*, 550.
6. Singh, A. K.; Kumar, P.; Yadav, M.; Pandey, D. S.; *J. Organomet. Chem.* **2010**, *695*, 567.
7. Dougan, S. J.; Melchart, M.; Habtemariam, A.; Parsons, S.; Sadler, P. J.; *Inorg. Chem.* **2006**, *45*, 10882.
8. Clarke, M. J.; *Coord. Chem. Rev.* **2002**, *232*, 69.
9. Lobana, T. S.; Kaur, P.; Castineira, S.; *J. Coord. Chem.* **2005**, *58*, 429.
10. Von Poelhsitz, G.; Bogado, A. L.; de Araujo, M. P.; Selistre-de-Araujo, H. S.; Ellena, J.; Castellano, E. E.; Batista, A. A.; *Polyhedron* **2007**, *26*, 4707.
11. Naal, Z.; Tfouni, E.; Benedetti, A. V.; *Polyhedron* **1994**, *13*, 133.
12. Massey, A.; Xu, Y. Z.; Karran, P.; *Curr. Biol.* **2001**, *11*, 1142.
13. Corral, E.; Hotze, A. C.; Den Dulk, H.; Leczkowska, A.; Rodger, A.; Hannon, M. J.; Reedijk, J.; *J. Biol. Inorg. Chem.* **2009**, *14*, 439.
14. Ramadan, S.; Hambley, T. V.; Kennedy, B. J.; Lay, P. A.; *Inorg. Chem.* **2004**, *43*, 2943.
15. Cini, R.; Tamasi, G.; Defazio, S.; Corsini, M.; Berrettini, F.; Cavaglioni, A.; *Polyhedron* **2006**, *25*, 834.
16. Constable, E. C.; King, A. C.; Palmer, C. A.; Raithby, P. R.; *Inorg. Chim. Acta* **1991**, *184*, 43.
17. Umakoshi, K.; Ichimura, A.; Kinoshita, I.; Ooi, S.; *Inorg. Chem.* **1990**, *29*, 4005.
18. Schmiedgen, R.; Huber, F.; Preud, H.; Ruisi, G.; Barbieri, R.; *Appl. Organomet. Chem.* **1994**, *8*, 397.
19. Gupta, M.; Cramer, R. E.; Ho, K.; Pettersen, C.; Mishina, S.; Belli, J.; Jensen, C. M.; *Inorg. Chem.* **1995**, *34*, 60.
20. Karagiannidis, P.; Aslanidis, P.; Kessissoglou, D. P.; Krebs, B.; Dartmann, M.; *Inorg. Chim. Acta* **1989**, *156*, 47.
21. Aslanidis, P.; Hadjikakou, S. K.; Karagiannidis, P.; Kojic-Prodic, B.; Luic, M.; *Polyhedron* **1994**, *13*, 3119.
22. Akrivos, P. D.; *Coord. Chem. Rev.* **2001**, *213*, 181.
23. Lang, E. S.; de Oliveira, G. M.; Casagrande, G. A.; Vázquez-López, E. M.; *Inorg. Chem. Commun.* **2003**, *6*, 1297.
24. Mcauliffe, C. A.; Mackie, A. G. In *Encyclopedia of Inorganic Chemistry*; King, R. B., ed.; Wiley: New York, 1994, pp. 2989.
25. Johnson, R. K.; Mirabelli, C. K.; Faucette, L. F.; McCabe, F. L.; Sutton, B. M.; Bryan, D. L.; Girard, G. R.; Hill, D. T.; *Proc. Am. Assoc. Cancer Res.* **1985**, *26*, 254.
26. Mirabelli, C. K.; Hill, D. T.; Faucette, L. F.; McCabe, F. L.; Girard, G. R.; Bryan, D. B.; Sutton, B. M.; Barus, J. O. L.; Crooke, S. T.; Johnson, R. K.; *J. Med. Chem.* **1987**, *30*, 2181.
27. Collins, L. A.; Franzblau, S. G.; *Antimicrob. Agents Chemother.* **1997**, *41*, 1004.
28. Palomino, J. C.; Martin, A.; Camacho, M.; Guerra, H.; Swings, J.; Portaels, F.; *Antimicrob. Agents Chemoter.* **2002**, *46*, 2720.
29. Mosmann, T. J.; *Immunol. Methods* **1983**, *65*, 55.
30. Quiroga, A. G.; Perez, J. M.; Lopez-Solera, I.; Montero, E. I.; Masaguer, J. R.; Alonso, C.; Navarro-Raninger, C.; *J. Inorg. Biochem.* **1998**, *69*, 275.
31. Marmor, J.; *J. Mol. Biol.* **1961**, *3*, 208.
32. Enraf-Nonius; Collect, Nonius BV, Delft: The Netherlands, 1997-2000.
33. Otwinowski, Z.; Minor, W. In *Macromolecular Crystallography*, Part A; Carter Jr., C. W.; Sweet, R. M., eds.; Academic Press: New York, 1997, pp. 307.
34. Blessing, R. H.; *Acta Crystallogr., Sect. A: Found. Crystallogr.* **1995**, *51*, 33.
35. Sheldrick, G. M.; *SHELXS-97, Program for Crystal Structure Resolution*; University of Göttingen, Göttingen, Germany, 1997.
36. Sheldrick, G. M.; *SHELXL-97, Program for Crystal Structures Analysis*; University of Göttingen, Göttingen, Germany, 1997.
37. Farrugia, L. J.; *J. Appl. Crystallogr.* **1997**, *30*, 565.
38. Parr, R. G.; Yang, W.; *Density-Functional Theory of Atoms and Molecules*; Oxford University Press: Oxford, 1989.
39. Frisch, M. J.; Trucks, G. W.; Schlegel, H. B.; Scuseria, G. E.; Robb, M. A.; Cheeseman, J. R.; Scalmani, G.; Barone, V.; Mennucci, B.; Petersson, G. A.; Nakatsuji, H.; Caricato, M.; Li, X.; Hratchian, H. P.; Izmaylov, A. F.; Bloino, J.; Zheng, G.; Sonnenberg, J. L.; Hada, M.; Ehara, M.; Toyota, K.; Fukuda, R.; Hasegawa, J.; Ishida, M.; Nakajima, T.; Honda, Y.; Kitao, O.; Nakai, H.; Vreven, T.; Montgomery, J. A., Jr.; Peralta, J. E.; Ogliaro, F.; Bearpark, M.; Heyd, J. J.; Brothers, E.; Kudin, K. N.; Staroverov, V. N.; Kobayashi, R.; Normand, J.; Raghavachari, K.; Rendell, A.; Burant, J. C.; Iyengar, S. S.; Tomasi, J.; Cossi, M.; Rega, N.; Millam, J. M.; Klene, M.; Knox, J. E.; Cross, J. B.; Bakken, V.; Adamo, C.; Jaramillo, J.; Gomperts, R.; Stratmann, R. E.; Yazyev, O.; Austin, A. J.; Cammi, R.; Pomelli, C.; Ochterski, J. W.; Martin, R. L.;

- Morokuma, K.; Zakrzewski, V. G.; Voth, G. A.; Salvador, P.; Dannenberg, J. J.; Dapprich, S.; Daniels, A. D.; Farkas, Ö.; Foresman, J. B.; Ortiz, J. V.; Cioslowski, J.; Fox, D. J.; *Gaussian 09*, Revision A.02; Gaussian, Inc., Wallingford, CT, 2009.
40. Hay, P. J.; Wadt, R. W.; *J. Chem. Phys.* **1985**, *82*, 270.
41. Stevens, W. J.; Basch, H.; Krauss, M.; *J. Chem. Phys.* **1984**, *81*, 6026.
42. Gordon, M. S.; *Chem. Phys. Lett.* **1980**, *76*, 163.
43. Egorova, M. B.; Dobrachenko, A. V.; Popov, A. M.; *Koord. Khim.* **1987**, *13*, 541.
44. Ma, G.; MacDonald, R.; Ferguson, M.; Cavell, R. G.; Patrick, B. O.; James, B. R.; Hu, T. Q.; *Organometallics* **2007**, *26*, 846.
45. Paim, L. A.; Dias, F. M.; Siebald, H. G. L.; Ellena, J.; Ardisson, J. D.; da Silva, M. M.; Batista, A. A.; *Polyhedron* **2012**, *42*, 110.
46. Krassowski, D. W.; Nelson, J. H.; Brower, K. R.; Hauenstein, D.; Jacobson, R. A.; *Inorg. Chem.* **1988**, *27*, 4294.
47. Batista, A. A.; Olmo, L. R. V.; Fontes, M. R. M.; Oliva, G.; *J. Braz. Chem. Soc.* **1996**, *7*, 257.
48. Corrêa, R. S.; Barolli, J. P.; Barbosa, M. I. F.; Ellena, J.; Batista, A. A.; *J. Mol. Struct.* **2013**, *1048*, 11.
49. Pinheiro, S. O.; de Sousa, J. R.; Santiago, M. O.; Carvalho, I. M. M.; Silva, A. L. R.; Batista, A. A.; Castellano, E. E.; Ellena, J.; Moreira, I. S.; Diogenes, I. C. N.; *Inorg. Chim. Acta* **2006**, *359*, 391.
50. Golfeto, C. C.; Von Poelhsitz, G.; Selistre-de-Araújo, H. S.; de Araujo, M. P.; Ellena, J.; Castellano, E. E.; Lopes, L. G. L.; Moreira, I. S.; Batista, A. A.; *J. Inorg. Biochem.* **2010**, *104*, 489.
51. Nakamoto, K.; *Infrared and Raman Spectra of Inorganic and Coordination Compounds*; Wiley: New York, 1986.
52. Martos-Calvente, R.; O'Shea, V. A. D.; Campos-Martin, J. M.; Fierro, J. L. G.; *J. Phys. Chem. A.* **2003**, *107*, 7490.
53. Mondelli, M. A.; Graminha, A. E.; Corrêa, R. S.; da Silva, M. M.; Carnizello, A. P.; Von Poelhsitz, G.; Ellena, J.; Deflon, V. M.; Caramori, G. F.; Torre, M. H.; Tavares, D. C.; Batista, A. A.; *Polyhedron* **2014**, *68*, 312.
54. Rao, C. N. R.; Venkataraghavan, R.; *Spectrochim. Acta* **1962**, *18*, 541.
55. Spinner, E.; *J. Chem. Soc.* **1960**, 1237.
56. Correa, R. S.; de Oliveira, K. M.; Delolo, F. G.; Alvarez, A.; Mocelo, R.; Plutin, A. M.; Cominetti, M. R.; Castellano, E. E.; Batista, A. A.; *J. Inorg. Biochem.* **2015**, *150*, 63.
57. Gallatti, T. F.; Bogado, A. L.; Von Poelhsitz, G.; Ellena, J.; Castellano, E. E.; Batista, A. A.; de Araujo, M. P.; *J. Organomet. Chem.* **2007**, *692*, 5447.
58. Pavan, F. R.; Von Poelhsitz, G.; do Nascimento, F. B.; Leite, S. R. A.; Batista, A. A.; Deflon, V. M.; Sato, N. D.; Franzblau, S. G.; Leite, C. Q. F.; *Eur. J. Med. Chem.* **2010**, *45*, 598.
59. dos Santos, E. R.; Mondelli, M. A.; Pozzi, L. V.; Corrêa, R. S.; Salistre-de-Araújo, H. S.; Pavan, F. R.; Leite, C. Q. F.; Ellena, J.; Malta, V. R. S.; Machado, S. P.; Batista, A. A.; *Polyhedron* **2013**, *51*, 292.
60. Barbosa, M. I. F.; Corrêa, R. S.; Pozzi, L. V.; Lopes, E. O.; Pavan, F. R.; Leite, C. Q. F.; Ellena, J.; Machado, S. P.; Von Poelhsitz, G.; Batista, A. A.; *Polyhedron* **2015**, *85*, 376.
61. Leite, G. G. S.; Baeza, L. C.; Batista, A. A.; Barbosa, M. I. F.; Pavan, F. R.; Leite, C. Q. F.; Silva, J. L.; Hirata, R. D. C.; Hirata, M. H.; Cardoso, R. F.; *Int. J. Microbiol. Res.* **2013**, *5*, 356.
62. Pyle, A. M.; Rehmann, J. P.; Meshoyrer, R.; Kumar, C. V.; Turro, N. J.; Barton, J. K.; *J. Am. Chem. Soc.* **1989**, *111*, 3051.

Submitted: June 22, 2015

Published online: September 15, 2015

FAPESP has sponsored the publication of this article.